Biointerface Research in Applied Chemistry
Platinum Open Access Journal (ISSN: 2069-5837)

Article
Volume 12, Issue 1, 2022, 529 - 536
https://doi.org/10.33263/BRIAC121.529536

Synthesis of WO_3 Nanoparticles using *Rhamnus Prinoides* Leaf Extract and Evaluation of its Antibacterial Activities

Asratemedhin B. Habtemariam [1,*], Yihun Alemu [1]

[1] Physics Department, College of Natural and Computational Sciences, Debre Berhan University, P. O. Box 445, Ethiopia
* Correspondence: asratemedhinbekele@dbu.edu.et (A.B.H.);

Scopus Author ID 57212268225

Received: 10.03.2021; Revised: 8.04.2021; Accepted: 12.04.2021; Published: 20.04.2021

Abstract: Tungsten trioxide (WO_3) is a transition metal oxide exhibiting unique properties suitable for various applications as in electrochromic devices, gas sensors, photocatalysis, and antimicrobial activities. Preparation of WO_3 nanostructures with controlled crystal structure and morphology is, thus, receiving greater attention. In this study, a facile and eco-friendly method was employed to successfully synthesis tungsten trioxide nanoparticles with monoclinic structure from *Rhamnus prinoides* plant leaf extract and sodium tungstate precursor. The obtained powder was characterized by X-Ray Diffraction (XRD), Scanning Electron Microscopy (SEM), and Fourier Transform Infrared (FTIR) spectroscopy. Antibacterial activities of the synthesized WO_3 nanoparticles were evaluated against Gram-positive and Gram-negative bacteria such as *Staphylococcus aureus*, *Listeria monocytogenes*, *Escherichia coli*, and *Salmonella typhimurium*.

Keywords: tungsten trioxide; nanoparticles; antibacterial activity; *Rhamnus prinoides.*

1. Introduction

Tungsten trioxide (WO_3) is a wide bandgap transition metal oxide semiconductor exhibiting a wide variety of novel properties useful for advanced technological applications [1,2]. WO_3 is a naturally existing oxide with less toxicity to living things and environmentally benign; chemically stable over a wider temperature range, and has unique electrical and optical properties, which renders its fascinating properties [2]. Commonly known applications of crystalline WO_3 nanoparticles include chemical sensing [3,4], biosensing [5], and photocatalysis [6-8]. Its antimicrobial activity against human pathogens has also been materialized in recent times [2,9,10].

Rhamnus prinoides L'Herit (*Rhamnus prinoides*) is an endemic plant to Ethiopia which grows to a height of about six meters, ecologically widespread, and locally cultivated from medium to high altitudes (1000-3200 m) [11]. It is commonly known as 'Gesho' (Amharic), and is widely planted in gardens [11,12]. In Ethiopia, *Rhamnus prinoides* are traditionally used to prepare alcoholic beverages, 'tella' and 'tej' (Amharic), and treat different kinds of bacterial infections. Intensive studies on *Rhamnus prinoides* revealed that it exhibits strong antioxidant properties due to polyphenols' presence in sufficient amounts [11]. Moreover, the antimicrobial activities of crude extracts from leaves, bark, and root of *Rhamnus prinoides* had been studied extensively [12,13].

So far, many different protocols have been employed for the synthesis of WO_3 nanoparticles, such as precipitation [10,14], hydrothermal [15-18], solution

combustion [19,20], spray pyrolysis [21], and biomimetic [22]. An alternative, inexpensive, and environmentally friendly technique for synthesizing metal oxide nanoparticles is the biological method that uses bacteria, fungi, or plant materials [23-26]. To the best of the researchers' knowledge, the synthesis of WO_3 nanostructures via plant extract has been attempted very recently [27]. This research successfully synthesized WO_3 nanoparticles from *Rhamnus prinoides* leaf extracts and evaluated their antibacterial activity against pathogenic bacteria (Staphylococcus aureus and Escherichia coli).

2. Materials and Methods

2.1. Materials and synthesis.

Analytical reagents such as sodium tungstate ($Na_2WO_4.2H_2O$, 99.99% purity) powder and hydrochloric acid (HCl, 30%) (Sigma Aldrich) were used without the need to purify further. Freshly collected, healthy leaves of *Rhamnus prinoides* (gesho) were taxonomically identified and cleaned with running water followed by distilled water. The leaves were shade dried for two weeks at room temperature until all moisture was lost. The dried leaves were then finely crushed and packed in a clean, transparent plastic bag and sealed until use.

Weighed 30 gm of *Rhamnus prinoides* leaves were boiled using 500 mL distilled water at 50 ºC for 1hour. The aqueous extract (pH of 5.9) was then cooled down to room temperature, filtered using Whatman No.1 filter paper, and stored at 4 °C for further use (Figure 1(a)). On the other hand, a 0.25 M solution of sodium tungstate was prepared by adding 82.5gm of the salt into 500 mL distilled water with continuous stirring while heating gently until the salt uniformly mix (Figure 1(b)).

In a typical synthesis procedure, 250 mL of aqueous leaf extract of *Rhamnus prinoides* was poured slowly into 250 mL of 0.25 M sodium tungsten precursor solution. The mixture was gradually heated at 100 ºC under continuous magnetic stirring for 1hour until the mixture color changes from brown to greenish (Figure 1(c)). The mixture mentioned above was then acidified by drop-wise addition of 5 mL HCl (30%) under continuous stirring until a greenish precipitate of $WO_3 \cdot nH_2O$ was obtained. The complete chemical reaction is as given in Equations (1) and (2) [1].

$$Na_2WO_4 \cdot 2H_2O + 2HCl + H_2O \rightarrow H_2WO_4 \cdot 3H_2O + 2NaCl \quad (1)$$

$$H_2WO_4 \cdot 3H_2O \rightarrow WO_3 + 4\,H_2O \quad (2)$$

After cooling down to room temperature, the resulting mixture was washed three times with distilled water after each centrifugation at 3500 rpm for 5 minutes to remove any unwanted impurities.

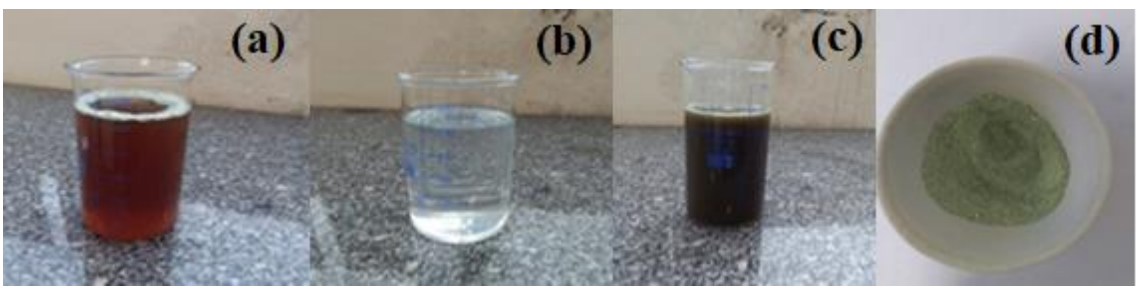

Figure 1. (**a**) Aqueous extract of *Rhamnus prinoides* leaf; (**b**) Sodium tungstate precursor solution; (**c**) Mixture of *Rhamnus prinoides* and precursor; (**d**) WO_3 nanopowder after annealing at 600 ºC.

Finally, the green precipitate was collected with a Petri dish and dried in a microwave oven at 100 ºC. The dried powder was then annealed under air at a temperature of 600 ºC [28] for 2 hours, and the resulting pale yellow powder, Figure 1(d), was carefully packed for the next characterization and application purposes.

2.2. Characterizations.

For phase identification, X-ray diffraction (XRD) patterns were recorded using an X-ray diffractometer, operating with CuKα radiation (λ=1.540598 Å) at a voltage of 40 kV and current of 30 mA. The XRD patterns of all randomly selected powder specimens were recorded in the 2θ range from 10° to 80° with a step size of 0.02 and a scan speed of 3°/min.

The average crystallite size 'D' was calculated from intense peaks using Scherrer's Equation (3).

$$D = \frac{k\,\lambda}{\beta \cos\theta}, \qquad (3)$$

where $'k'$ is the Scherrer's shape factor with value 0.9, 'λ' is the wavelength of radiation, $'\beta'$ is the full width at half maximum (FWHM) and $'\theta'$ is the diffraction angle.

The lattice parameters for the monoclinic structure were calculated from the powder XRD pattern using Equation (4):

$$\frac{1}{d^2} = \frac{1}{sin^2\ \beta}\left(\frac{h^2}{a^2} + \frac{l^2}{c^2} - \frac{2\,hl\,cos\beta}{ac}\right) + \frac{k^2}{b^2}, \qquad (4)$$

where '*a*', '*b*' and '*c*' are lattice parameters, '*d* ' is the inter-planar spacing, and '*h*', '*k*', '*l*' are miller's indices.

Fourier-transform infrared instrument having the range of 4000cm^{-1} to 400cm^{-1} was used to record spectral analysis. Morphological studies of WO_3 nanorods synthesized from *Rhamnus prinoides* leaf extract were analyzed by scanning electron microscopy, SEM model JSM-IT300LV, in the micrometer scale.

2.3. Phytochemical test of Rhamnus prinoides.

The presence of bioactive compounds in the leaf extract of *Rhamnus prinoides* was examined, and the result is shown in Table 1.

Table 1. Phytochemical test of *Rhamnus prinoides*.

Alkaloids	Tannins	Flavonoid	Saponin	Terpenoids	Steroids	Glycosides
++	+	+	+	+	+	++

++ = Strong presence of component and + = presence of component.

2.4. Antimicrobial activity.

The antibacterial activity of WO_3 nanoparticles was tested for Gram-positive and Gram-negative bacteria using the agar well diffusion method. *Listeria monocytopens* (Lm) and staphylococcus aureus (Sa) were taken as Gram-positive bacterial. Salmonella typhimurium (St) and Escherichia coli (Ec) were taken as Gram-negative bacteria. *Candida albicans* (Ca) was yeast which was extracted from the patient. *Escherichia coli*, a broad-spectrum antibiotic, was used as control.

To study the antimicrobial activity, the synthesized WO_3 powder was first dispersed in the solvent. The microbial was grown in nutrient broth culture by incubating at 37 ºC for 24 hours. It was then transferred into a Petri dish coated with Muller Hinton Agar with the help of a paper disk. The powder's different concentrations were applied to the Gram-negative and

Gram-positive microbial in the petri dish at 37 ºC followed by 24 hours incubation. Finally, inhibition diameter measurement was carried out.

3. Results and Discussion

3.1. Powder X-ray diffraction (XRD).

For phase identification and crystallinity study of the synthesized nanoparticles, XRD characterization of the powder sample annealing at 600 ºC was used. The XRD peaks, Figure 2, which appeared at 2θ = 23.15º, 23.66º, 24.36º, 26.65º, 28.35º, 33.31º, 34.18º, 35.61º, 41.93º, 47.24º, 48.34º, 50.04º, 56.60º, 62.28º corresponds to miller indices (0 0 2), (0 2 0), (200), (120), (1 1 1), (0 2 1), (220), (121), (221), (002), (040), (140), (141), and (340), respectively.These peaks are indexed to the monoclinic crystal structure of WO_3 as confirmed by JCPDS card no.00-020-1324.

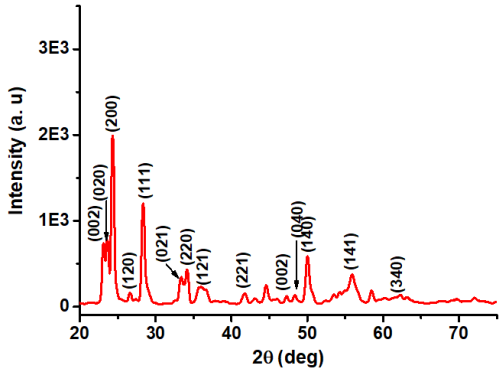

Figure 2. XRD patterns of biosynthesized WO_3 nanoparticles annealed at 600 ºC.

The average crystallite size was calculated from prominent peaks with miller indices (200), (111), (140), and (141) using Equation (3) to be 60 nm.

3.2. Fourier-transform infrared (FTIR) spectroscopy.

FTIR spectrum of *Rhamnus prinoides* plant extract was taken before annealing the powder sample. The band at 3668.3 cm^{-1} was assigned to the O–H stretching vibration of *Rhamnus prinoides* plant extract [15]. The peaks at the wavenumber of 2983.2 cm^{-1} and 2902.4 cm^{-1} are assigned to the anti-symmetric stretching vibrations of the $–CH_2–$ and $–CH_3$ group present in the carbon chain of the plant [15]. In Figure 3(a), the peaks at 1722.6 cm^{-1}, 1605.8 cm^{-1}, 1389.4 cm^{-1}, 1327.4 cm^{-1}, 1216.4 cm^{-1} and 1116.1 cm^{-1} are also O–H stretching and bending modes [15].

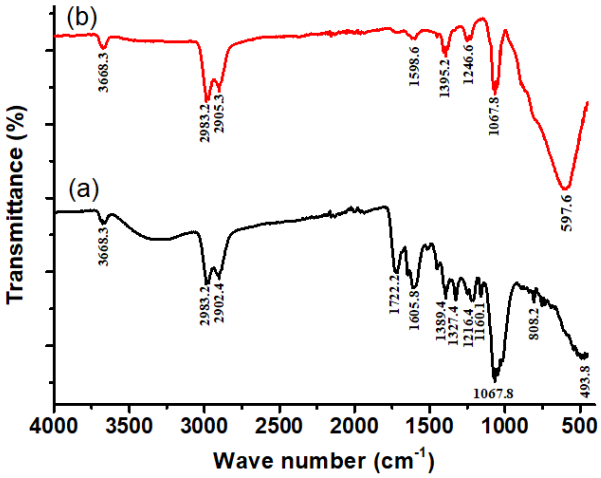

Figure 3. FTIR spectrum of (**a**) *Rhamnus prinoides* extract; (**b**) WO_3 nanoparticles.

The sharp peaks at 1067.8 cm^{-1} and 493.8 cm^{-1} are related to the WO-OH. FTIR spectrum of WO_3 nanopowder, Figure 3(b), was indexed to 3668.3 cm^{-1}, 2983.2 cm^{-1}, 2905.3 cm^{-1}, 1395.2 cm^{-1}, 1246.6 cm^{-1}, 1067.8 cm^{-1} and 597.6 cm^{-1}. The sharp peak at 597.6 cm^{-1} is attributed to the O–W–O stretching vibration mode [29].

3.3. Scanning electron microscope (SEM).

SEM micrograph analysis of the synthesized tungsten trioxide nanoparticles after calcinating at 600 ºC was recorded. Figure 4 shows the particle size distribution, which reveals the formation of spherical shapes nanoparticles. The crystallite size of the synthesized tungsten trioxide nanoparticles is in the range of 60 nm. Imagej was utilized to calculate the average crystallite size, and it was confirmed by the XRD result.

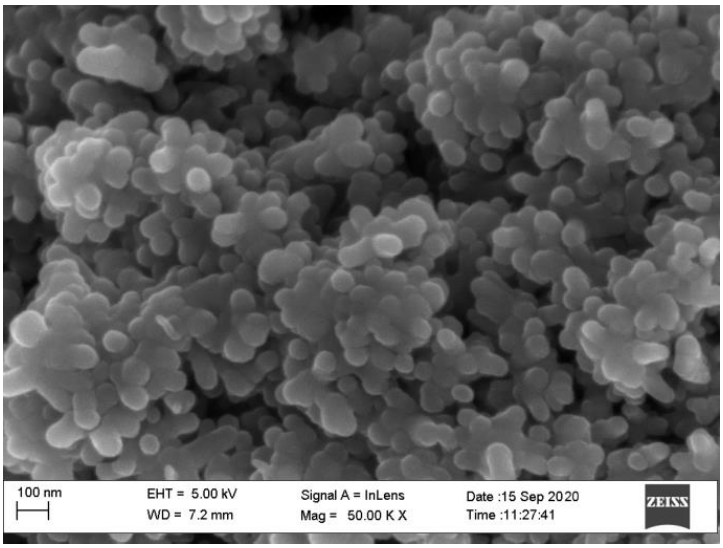

Figure 4. SEM images of biosynthesized WO_3 nanoparticles.

3.4. Antibacterial activity.

The synthesized WO_3 nanoparticles exhibited strong antibacterial activity for both 250mg/mL and 125 mg/mL concentrations. As shown in Figure 5, the inhibition zone was measured for *Listeria monocytopens* (Lm), *Staphylocous aureus* (Sa), *Salmonella typhimurium* (Sa), and *Escherichia coli* (Ec) and *Candida albicans* (Ca) in agreement with previous findings [9,10].

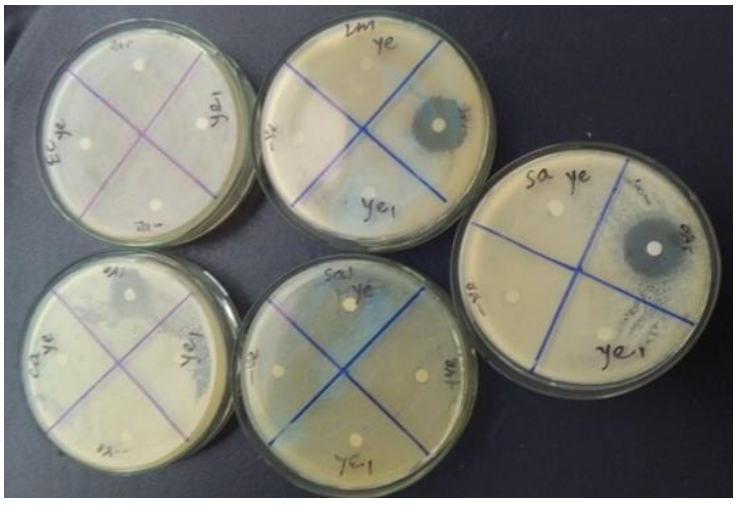

Figure 5. Antibacterial activity of WO_3 powder on S. aureus and E. coli bacterial strains.

4. Conclusions

In conclusion, spherical tungsten trioxide nanoparticles exhibiting monoclinic phase were successfully synthesized through the biological synthesis method from sodium tungstate precursor and *Rhamnus prinoides* leaf extract. Antimicrobial studies of the as-synthesized nanoparticles show significantly observable bacterial growth inhibition.

Funding

This research received no external funding.

Acknowledgments

The researchers are thankful to the Institute of letter technology for FTIR characterization and the Materials Science and Engineering Department at Adama Science and Technology University for running XRD characterization.

Conflicts of Interest

The authors declare no conflict of interest.

References

1. Ahmadi, M.; Younesi, R.; Guinel, M. J.-F. Synthesis of tungsten oxide nanoparticles using a hydrothermal method at ambient pressure. *Journal of Materials Research* **2014**, *29*, 1424-1430. https://doi.org/10.1557/jmr.2014.155.
2. Mardare, C. C.; Hassel, A. W. Review on the versatility of tungsten oxide coatings. *physica status solidi (a)* **2019**, *216*, 1900047. https://doi.org/10.1002/pssa.201900047.
3. Ramanavičius, S.; Petrulevičienė, M.; Juodkazytė, J.; Grigucevičienė, A.; Ramanavičius, A. Selectivity of tungsten oxide synthesized by sol-gel method towards some volatile organic compounds and gaseous materials in a broad range of temperatures. *Materials* **2020**, *13*, 523. https://doi.org/10.3390/ma13030523.
4. Galstyan, V.; Poli, N.; D'Arco, A.; Macis, S.; Lupi, S.; Comini, E. A novel approach for green synthesis of WO_3 nanomaterials and their highly selective chemical sensing properties. *Journal of Materials Chemistry A* **2020**, *8*, 20373-20385. https://doi.org/10.1039/D0TA06418A.
5. Santos, L.; Silveira, C. M.; Elangovan, E.; Neto, J. P.; Nunes, D.; Pereira, L.; Martins, R.; Viegas, J.; Moura, J. J.; Todorovic, S; Almeida, M. G; Fortunato, E. Synthesis of WO_3 nanoparticles for biosensing applications. *Sensors and Actuators B: Chemical* **2016**, *223*, 186-194. https://doi.org/10.1016/j.snb.2015.09.046.
6. Sirotkin, N.; Khlyustova, A.; Titov, V.; Krayev, A.; Nikitin, D.; Dmitrieva, O.; Agafonov, A. Synthesis and Photocatalytic Activity of WO_3 Nanoparticles Prepared by Underwater Impulse Discharge. *Plasma Chemistry and Plasma Processing* **2020**, *40*, 571-587. https://doi.org/10.1007/s11090-019-10048-z.
7. Rong, R.; Wang, L. Synthesis of hierarchical hollow nest-like WO_3 micro/nanostructures with enhanced visible light-driven photocatalytic activity. *Journal of Alloys and Compounds* **2021**, *850*, 156742. https://doi.org/10.1016/j.jallcom.2020.156742.
8. Aslam, I.; Farooq, M. H.; Iqbal, M.; Boddula, R.; Abid, M.; Ashfaq, M.; Ghani, U. Synthesis of $WO_3 \cdot H_2O$ spherical particles for efficient photocatalytic properties under visible light source. *Materials Science for Energy Technologies* **2019**, *2*, 187-193. https://doi.org/10.1016/j.mset.2019.02.002.
9. Duan, G.; Chen, L.; Jing, Z.; De Luna, P.; Wen, L.; Zhang, L.; Zhao, L.; Xu, J.; Li, Z.; Yang, Z.; Zhou, R.; Robust antibacterial activity of tungsten oxide (WO_{3-X}) nanodots. *Chemical research in toxicology* **2019**, *32*, 1357-1366. https://doi.org/10.1021/acs.chemrestox.8b00399.
10. Baig, U.; Gondal, M. A.; Rehman, S.; Akhtar, S. Facile synthesis, characterization of nano-tungsten trioxide decorated with silver nanoparticles and their antibacterial activity against water-borne gram-negative pathogens. *Applied Nanoscience* **2020**, *10*, 851-860. https://doi.org/10.1007/s13204-019-01186-z.

11. Chen, G.L.; Munyao Mutie, F.; Xu, Y.-B.; Saleri, F. D.; Hu, G.-W.; Guo, M..Q.; Guo, M.Q.; Antioxidant, anti-inflammatory activities and polyphenol profile of Rhamnus prinoides. *Pharmaceuticals* **2020**, *13*, 55. https://doi.org/10.3390/ph13040055.
12. Campbell, M.; Zhao, W.; Fathi, R.; Mihreteab, M.; Gilbert, E. S. Rhamnus prinoides (gesho): A source of diverse anti-biofilm activity. *J. Ethnopharmacol.* **2019**, *241*, 111955. https://doi.org/10.1016/j.jep.2019.111955.
13. Molla, Y.; Nedi, T.; Tadesse, G.; Alemayehu, H.; Shibeshi, W. Evaluation of the in vitro antibacterial activity of the solvent fractions of the leaves of Rhamnus prinoides L'Herit (Rhamnaceae) against pathogenic bacteria. *BMC complementary and alternative medicine* **2016**, *16*, 1-9. https://doi.org/10.1186/s12906-016-1279-6.
14. Martínez-de la Cruz, A.; Martínez, D. S.; Cuéllar, E. L. Synthesis and characterization of WO_3 nanoparticles prepared by the precipitation method: evaluation of photocatalytic activity under vis-irradiation. *Solid State Sciences* **2010**, *12*, 88-94. https://doi.org/10.1016/j.solidstatesciences.2009.10.010.
15. Adhikari, S.; Sarkar, D.; Maiti, H. S. Synthesis and characterization of WO_3 spherical nanoparticles and nanorods. *Materials Research Bulletin* **2014**, *49*, 325-330. https://doi.org/10.1016/j.materresbull.2013.08.028.
16. Tehrani, F. S.; Ahmadian, H.; Aliannezhadi, M. Hydrothermal synthesis and characterization of WO_3 nanostructures: effect of reaction time. *Materials Research Express* **2020**, *7*, 015911. https://doi.org/10.1088/2053-1591/ab66fc.
17. Ahmadian, H.; Tehrani, F. S.; Aliannezhadi, M. Hydrothermal synthesis and characterization of WO_3 nanostructures: effects of capping agent and pH. *Materials Research Express* **2019**, *6*, 105024. https://doi.org/10.1088/2053-1591/ab3826.
18. Nagyné-Kovács, T.; Lukács, I. E.; Szabó, A.; Hernadi, K.; Igricz, T.; László, K.; Szilágyi, I. M.; Pokol, G. Effect of pH in the hydrothermal preparation of monoclinic tungsten oxide. *Journal of Solid State Chemistry* **2020**, *281*, 121044. https://doi.org/10.1016/j.jssc.2019.121044.
19. Aliasghari, H.; Arabi, A.; Haratizadeh, H. A novel approach for solution combustion synthesis of tungsten oxide nanoparticles for photocatalytic and electrochromic applications. *Ceramics International* **2020**, *46*, 403-414. https://doi.org/10.1016/j.ceramint.2019.08.275.
20. Liu, Z.; Li, P.; Dong, Y.; Wan, Q.; Zhai, F.; Volinsky, A. A.; Qu, X. Facile preparation of hexagonal $WO_3{\cdot}0.33H_2O$/C nanostructures and its electrochemical properties for lithium-ion batteries. *Applied surface science* **2017**, *394*, 70-77. https://doi.org/10.1016/j.apsusc.2016.10.107.
21. Nakakura, S.; Arif, A. F.; Rinaldi, F. G.; Hirano, T.; Tanabe, E.; Balgis, R.; Ogi, T. Direct synthesis of highly crystalline single-phase hexagonal tungsten oxide nanorods by spray pyrolysis. *Advanced Powder Technology* **2019**, *30*, 6-12. https://doi.org/10.1016/j.apt.2018.09.040.
22. Uchiyama, H.; Mizuguchi, S.; Hirano, S. Biomimetic synthesis of nanostructured $WO_3{\cdot}H_2O$ particles and subsequent thermal conversion to WO_3. *Royal Society open science* **2019**, *6*, 182137. https://doi.org/10.1098/rsos.182137.
23. Vasantharaj, S.; Sathiyavimal, S.; Senthilkumar, P.; Oscar, F. L.; Pugazhendhi, A. Biosynthesis of iron oxide nanoparticles using leaf extract of Ruellia tuberosa: Antimicrobial properties and their applications in photocatalytic degradation. *J. Photochem. Photobiol., B: Biology* **2019**, *192*, 74-82. https://doi.org/10.1016/j.jphotobiol.2018.12.025.
24. Habtemariam, A. B.; Sibhatu, A. K.; Weldegebrieal, G. K.; Zelekew, O. A.; Tekletsadik, B. T. Bio-mediated synthesis of ZnO nanostructures from Thymus Schimperi leaves extract and its antibacterial and photocatalytic activities. *Letters in Applied NanoBioScience* **2020**, *9*, 808-813. https://doi.org/10.33263/LIANBS91.808813.
25. Yadi, M.; Mostafavi, E.; Saleh, B.; Davaran, S.; Aliyeva, I.; Khalilov, R.; Nikzamir, M.; Nikzamir, N.; Akbarzadeh, A.; Panahi, Y. Current developments in green synthesis of metallic nanoparticles using plant extracts: a review. *Artificial cells, nanomedicine, and biotechnology* **2018**, *46*, S336-S343. https://doi.org/10.1080/21691401.2018.1492931.
26. Aisida, S. O.; Madubuonu, N.; Alnasir, M. H.; Ahmad, I.; Botha, S.; Maaza, M.; Ezema, F. I. Biogenic synthesis of iron oxide nanorods using Moringa oleifera leaf extract for antibacterial applications. *Applied Nanoscience* **2020**, *10*, 305-315. https://doi.org/10.1007/s13204-019-01099-x.
27. Tijani, J.; Ugochukwu, O.; Fadipe, L.; Bankole, M.; Abdulkareem, A.; Roos, W. One-step green synthesis of WO_3 nanoparticles using Spondias mombin aqueous extract: effect of solution pH and calcination temperature. *Appl. Phys. A* **2019**, *125*, 162. https://doi.org/doi:10.1007/s00339-019-2450-y.
28. Bourdin, M.; Gaudon, M.; Weill, F.; Duttine, M.; Gayot, M.; Messaddeq, Y.; Cardinal, T. Nanoparticles (NPs) of WO_{3-x} compounds by polyol route with enhanced photochromic properties. *Nanomaterials* **2019**, *9*, 1555. https://doi.org/doi:10.3390/nano9111555.

29. Rezaee, O.; Chenari, H. M.; Ghodsi, F. Precipitation synthesis of tungsten oxide nanoparticles: X-ray line broadening analysis and photocatalytic efficiency study. *Journal of Sol-Gel Science and Technology* **2016**, *80*, 109-118. https://doi.org/doi:10.1007/s10971-016-4073-5.